European Conferences on Biomedical Optics 2021 (ECBO) © OSA-SPIE 2021

Evaluating a new generation of wearable high-density diffuse optical tomography (HD-DOT) technology via retinotopic mapping in the adult brain

Ernesto E. Vidal-Rosas[a], Hubin Zhao[a,b], Reuben Nixon-Hill[c,d], Greg Smith[c], Luke Dunne[d], Samuel Powell[c,e], Robert J. Cooper[a], and Nicholas L. Everdell[c]

[a]*DOT-HUB, BORL, Department of Medical Physics and Biomedical Engineering, University College London, London, WC1E 6BT, UK*
[b]*James Watt School of Engineering, University of Glasgow, Glasgow, G12 8QQ, UK*
[c]*Gowerlabs Ltd., London, UK*
[d]*Department of Mathematics, Imperial College London, London, SW7 2BU, UK*
[e]*Department of Electrical and Electronic Engineering, Nottingham University, Nottingham, NG7 2RD, UK*
ernesto.vidal@ucl.ac.uk

Abstract: We investigated the performance of a novel HD-DOT system by replicating a series of classic visual stimulation paradigms. Haemodynamic response functions and cortical activation maps replicated the results obtained with larger fibre-based systems.

1. Introduction

The investigation of the human brain function has shown dramatic progress due to the development of functional neuroimaging. Traditional functional magnetic resonance imaging (fMRI) and positron emission tomography (PET) have led the advance. However, they are not free of limitations including the costs associated and the restrictions on mobility which makes the study of populations such as infants very difficult. Diffuse optical methods have shown great potential in overcoming many of these challenges. In recent years, high-density diffuse optical tomography (HD-DOT) has been shown to approach the resolution and localization accuracy of BOLD-fMRI in the adult brain by exploiting densely spaced, overlapping samples of the probed tissue volume [1, 2]. One limitation is that the technique has to-date required large and cumbersome optical fibre arrays and as a consequence, the studies have been restricted to the laboratory space. In this work, we evaluate a new HD-DOT system that offers the possibility of minimally constrained brain imaging. We investigated the performance of the system by employing a battery of classical visual paradigms. The visual cortex has been extensively studied and has been used to validate fMRI, PET and fibre-based HD-DOT systems [3-5].

2. Materials and methods

2.1. Wearable HD-DOT system

The HD-DOT device is a 12-module LUMO system (Gowerlabs Ltd., UK) which consists of multiple, independent hexagonal modules (Fig. 1a), each containing four photodiodes and three dual-wavelength LEDs emitting at 735 nm and 850 nm. The system builds upon the principle of modularity [6] and offers extensive flexibility to organise the modules to suit the experimental paradigm while conforming to the head's curvature. Fig. 1b shows the full arrangement that yields a total of 1728 dual-wavelength source-detector channels.

2.2. Subject and experimental protocol

The study considered a single, healthy participant (author RJC, male, 36 years old) and comprised fifteen sessions in a period of three weeks and under lockdown conditions due to the COVID-19 outbreak. Each experiment took place in a quiet and dimly lit room where the participant fitted himself with the neoprene cap and sat in an adjustable chair in front of a 27-inch computer monitor at a viewing distance of 90 cm. The participant then started a computer program that automatically controlled the display of the different stimuli and simultaneously controlled a webcam (1080p, Fusion5 Ltd.) to record the front view of the participant for quality control and attention monitoring purposes.

The protocol included two visual stimulation paradigms. First, a polar angle mapping which consisted of a radial black and white grid rotating clockwise at 10°/s for a full cycle of 36 s (Fig. 1c). Second, a visual eccentricity experiment which consisted of a black and white grid (reversing at 10 Hz) presented at the center or periphery and on the right or the left of the visual field (Fig. 1d). Each paradigm lasted a total of 19 minutes.

2.3. 3D head modelling and registration

The 3D digitization of the optode locations was performed using photogrammetry. The process started by having a second individual to record a video of the participant's head using a smartphone (iPhone XR, Apple Inc.). The video was directly imported into a commercial software package (Metashape, Agisoft LLC) to produce a 3D model of the head (fig. 1e). The location of the sources and detectors was found with the aid of green triangular markers. Finally, these locations were mapped into a subject-specific finite element model obtained from MRI scans (Fig. 1f).

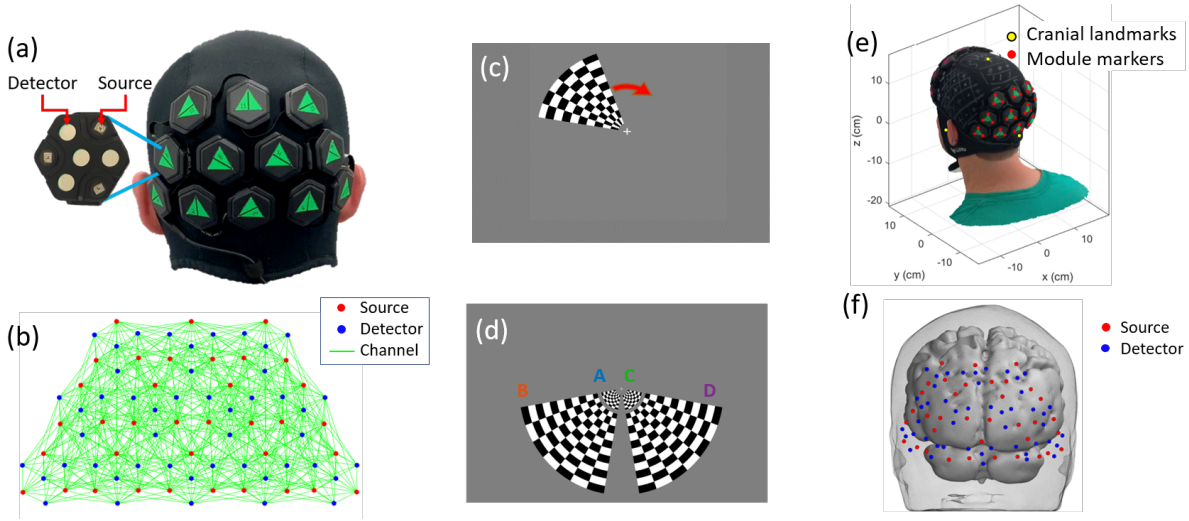

Fig. 1 (a) 12-module LUMO system. (b) The total number of available logic channels (1728 dual-wavelength channels). (c) Polar angle stimulus. (c) Eccentricity stimuli. (e) 3D model of the participant's head obtained from a photogrammetry process (f) 3D model used for image reconstruct.

3. Results and discussion

Figure 2a shows a frame of the change in oxygenated haemoglobin (ΔHbO) during the presentation of the rotation stimulus, the point of maximum ΔHbO is indicated with the green circle. Figure 2b is the time series of oxy-, deoxy- (ΔHbR) and total-haemoglobin (ΔHbT) changes at the location of maximum ΔHbO, each time the rotating stimulus activates this point there is a maximum increase in ΔHbO. Figure 2c is a group average phase map that relates the angle of the rotating wedge with a particular region of the visual cortex [7].

Figure 2d shows the haemodynamic response due to a central left stimulus in the channel space in one session, this figure also highlights the large number of channels available for image reconstruction. Figures 2e-f show the 3D reconstructions of ΔHbO and ΔHbR, respectively. These maps show distinct and robust activations in the hemisphere contralateral to the stimulus. Figures 2g-j show the grand average ΔHbO for each condition. The central activations achieved higher concentration change values in comparison to the peripheral stimuli. Figures 2k-n show the sum of binary maps of ΔHbO response across sessions for each condition. Each map represents the number of sessions in which a node location lies within 50% of the maximum HbO response. Note the high number of coincident points for all conditions, demonstrating the consistency of the haemodynamic changes across sessions obtained with the system. These results show that high density data improves repeatability, robustness, and spatial resolution. Our results are in agreement with those results obtained with larger fibre-based DH-DOT systems [2, 5, 7].

4. Conclusion

We demonstrate the performance of a wearable HD-DOT system by replicating a series of classical visual paradigms that have been used extensively with fibre-based HD-DOT and undertaking multiple comparisons in a single, highly imaged individual. Our results show that the location accuracy, magnitude, and spatial extent of the activation maps that can be obtained with this device are comparable to those of larger, fibre-based HD-DOT systems. The study also demonstrated that these measurements can be obtained with ease, even self-applied in a home setting. This presents a crucial advance towards minimally constrained brain imaging that will make it possible to investigate cognitive function not only in the laboratory but also in ecologically valid settings.

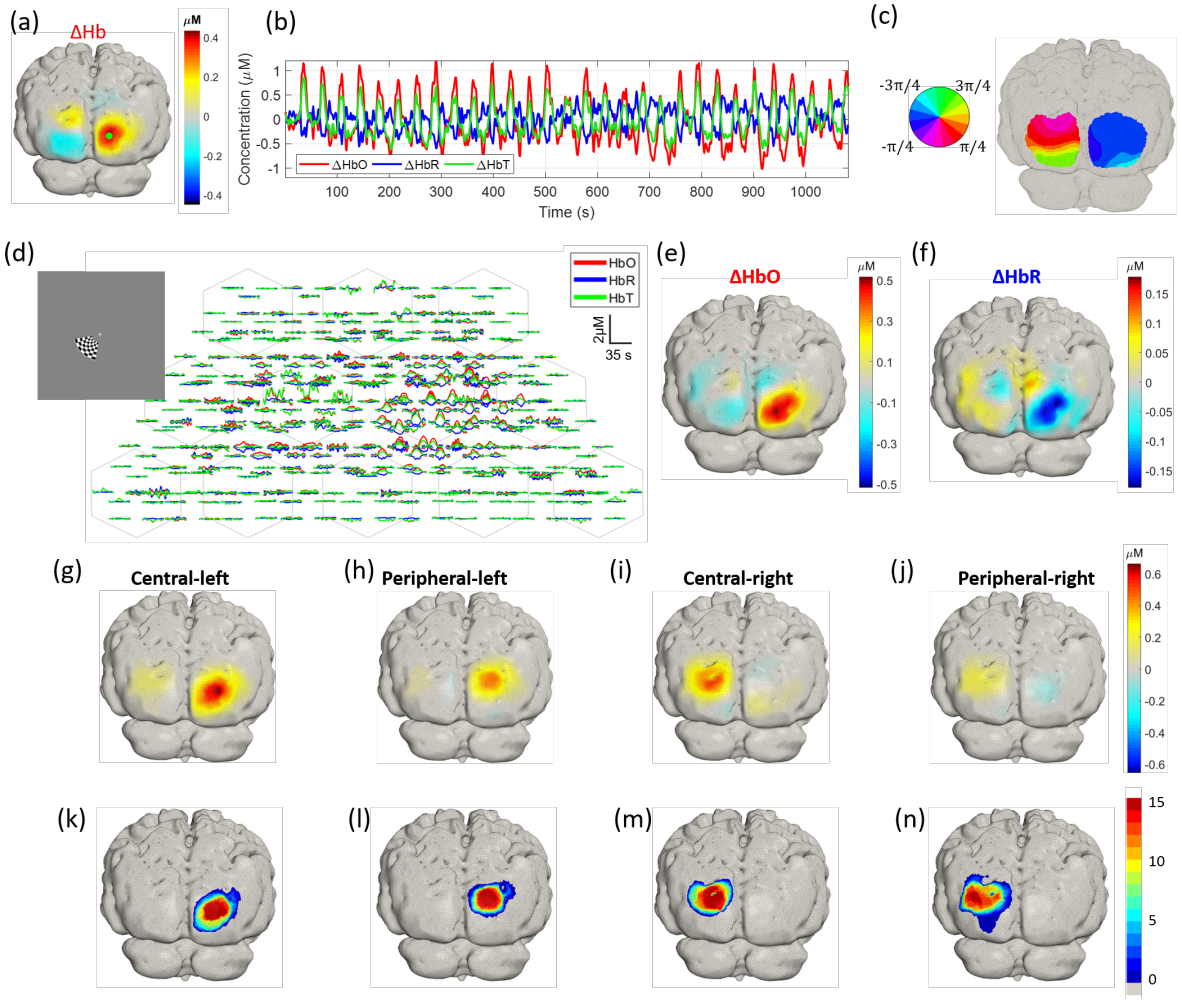

Fig. 2 (a) Example of one frame of the activation map for a single session obtained from the rotating wedge stimulus. (b) Temporal evolution of the haemodynamic response relative to the average of the full length of the rotation experiment in one single session for the point of maximum ΔHbO (green points in (a)). (c) Phase data obtained from the Fourier transform of the time-series at each node location at a group level. (d) Example of single-session hemodynamic response functions for a left central stimulus plotted in the channel space. The stimulus is displayed in the inset on the top left corner. (e)-(f) The corresponding reconstructed ΔHbO and ΔHbR images projected into the grey matter mesh. (g)-(j) Group average ΔHbO across all sessions for each condition. (k)-(n) Overlap of activations ΔHbO for each condition.

5. References

[1] A. T. Eggebrecht et al., "Mapping distributed brain function and networks with diffuse optical tomography," Nat. Photonics, vol. 8, no. 6, pp. 448–454, May 2014.

[2] A. T. Eggebrecht et al., "A quantitative spatial comparison of high-density diffuse optical tomography and fMRI cortical mapping," Neuroimage, vol. 61, no. 4, pp. 1120–1128, 2012.

[3] P. T. Fox et al., "Retinotopic organization of human visual cortex mapped with positron-emission tomography," J. Neurosci. (1987)

[4] S. A. Engel et al., "FMRI of human visual cortex," in Nature (1994)

[5] B. W. Zeff, B. R. White, H. Dehghani, B. L. Schlaggar, and J. P. Culver, "Retinotopic mapping of adult human visual cortex with high-density diffuse optical tomography," Proc. Natl. Acad. Sci., 2007.

[6] D. Chitnis et al., "Functional imaging of the human brain using a modular, fibre-less, high-density diffuse optical tomography system," Biomed. Opt. Express, 2016.

[7] B. R. White and J. P. Culver, "Phase-encoded retinotopy as an evaluation of diffuse optical neuroimaging," Neuroimage, 2010.